RSC Advances

PAPER

View Article Online
View Journal | View Issue

Cite this: *RSC Adv.*, 2025, **15**, 34821

A new multi-purpose FRET fluorescent probe for the simultaneous detection of proteases

Petra Jedináková,[a] Zuzana Barbuščáková,[a] David Milićević,[a] Martin Kubala[b] and Jan Hlaváč *[a]

A new methodology for the detection of three model proteases using a multi-purpose peptide probe equipped with three selectively cleavable sites and four fluorophores was developed and studied. The probe was designed as a single-excitation, triple-emission system, allowing for the monitoring of characteristic real-time changes in the fluorescence emission responses of individual fluorophores during enzymatic cleavage. It was labelled with diethylaminocoumarin (DEAC), fluorescein (FL) and Rhodamine B (RhB), forming the DEAC → FL → RhB FRET-cascade, with estimated Förster distances of 3.08 ± 0.02 nm or 3.02 ± 0.02 nm for the DEAC → FL FRET-pair (depending on the DEAC labeling site) and 6.04 ± 0.05 nm for the FL → RhB FRET-pair. Although spectroscopic analyses indicate that photophysical processes other than FRET are involved in the probe, the huge changes in its fluorescence intensities (*e.g.*, the fluorescence intensity of the probe for the excitation/emission wavelengths 421 nm/476 nm is 50-fold lower compared to that of the DEAC-only labeled construct, or it is 200-fold lower for 480 nm/521 nm compared to that of the FL-only labeled construct) enable the easy detection of protease activities. In a single-enzyme mode, trypsin, chymotrypsin, and thrombin can be determined according to the ratiometric graphical model at the lowest detectable concentrations of 0.0625 ng mL^{-1}, 0.125 μg mL^{-1}, and 0.0125 U mL^{-1}, respectively. The prepared probe, in combination with selective inhibitors (Kunitz, trypsin inhibitor; chymostatin, chymotrypsin inhibitor; and dabigatran, thrombin inhibitor), was also successfully used for the simultaneous detection of individual proteases in their two-enzyme mixtures. Finally, the probe was studied as a tool for three-protease screening using two selected inhibitors. Unfortunately, a universal model capable of unambiguous confirmation of the three studied enzymes in various combinations of their quantities has not been found.

Received 5th May 2025
Accepted 1st September 2025

DOI: 10.1039/d5ra03163j

rsc.li/rsc-advances

Introduction

In living organisms, proteases play a critical role in multiple biological processes, including DNA replication and transcription, cell proliferation and differentiation, hemostasis, blood coagulation, inflammation, immunity, necrosis, and apoptosis.[1] An imbalance in protease activity can be linked to a variety of pathological states, such as cancer, diabetes, inflammation, vascular diseases, and Alzheimer's disease.[2,3] Monitoring protease activities is essential for understanding the relationship between proteases and diseases, as well as for the elucidation of metabolic pathways; thus, extensive efforts have been undertaken to develop sensitive, selective, and robust assays for protease detection.[3,4]

Protease assays can be classified as homogenous and heterogenous.[4,5] Most obvious homogenous assays are further classified into colorimetric assays, mass spectrometry-based assays, fluorescence (or Förster) resonance energy transfer assays, and assays using nanoparticles such as noble metal nanoparticles, quantum dots, and graphene oxide.[4] Peptide fragments obtained by homogenous assays are usually separated by liquid chromatography and detected by UV, fluorescence, or mass spectrometry. The main disadvantage of this approach is that it allows only end-pointed measurements and expensive instrumentation.[4] However, spectral monitoring, such as FRET-based detection techniques, enables a real-time protease assay with cheap and readily available materials. In general, FRET probes consist of a short peptide connecting a FRET donor and FRET acceptor, which range from organic molecules to nanomaterials and quantum dots.[4]

Many FRET peptide probes for the detection of a single protease have been developed and described in recent reviews covering this area.[3,4,6] There also exist examples describing FRET systems for the simultaneous detection of two proteases. In 2006, Wu and co-workers described the first FRET-based probe for the simultaneous detection of caspase-3 and caspase-6.[7] Nearly a decade later, Li and co-workers synthesized

[a]*Department of Organic Chemistry, Faculty of Science, Palacký University Olomouc, 17. Listopadu 12, 771 46 Olomouc, Czech Republic. E-mail: jan.hlavac@upol.cz*
[b]*Department of Experimental Physics, Faculty of Science, Palacký University Olomouc, 17. Listopadu 12, 771 46 Olomouc, Czech Republic*

a probe for the sequential detection of MMP2 and caspase-3,[8] followed by the FRET probe for the simultaneous imaging of MMP2 and caspase-3.[9] In 2018, FRET-based dual probe for the simultaneous detection of human thrombin and MMP activity was developed in Bradley's group.[10] Cheng and co-workers synthesized a dual-colour fluorescent probe for the visualization of main protease (M^{PRO}) and papain-like protease (PL^{PRO}), which play a critical role in SARS-CoV-2 replication.[11] All these systems use a quencher to keep the intact probe switched off before cleavage, which does not allow for monitoring its penetration, organelle accumulation, *etc.* Multi-FRET ratiometric probes for the simultaneous detection of trypsin and chymotrypsin,[12] as well as caspase-8 and caspase-9 (ref. 13) or with "always-ON" fluorescent properties have been developed by our group. Additionally, systems for the identification of more different species have been developed previously by our group.[14,15] Biosensors based on semiconductor quantum dots and FRET have been widely studied by several groups developing systems for tracking multiple proteases or different species.[14–20] The main drawbacks of these systems include a time-consuming calibration/evaluation process and potential QD-induced cytotoxicity, which is also discussed.[21] For fluorescent detection of three or more proteases, only few model systems have been described to date. In 2013, Huang and co-workers published an article that described a carbon nanotube-based fluorescent peptide probe for the simultaneous detection of MMP7, MMP2, and urokinase-type plasminogen activator (uPA).[22] Xu and co-workers developed a peptide-based four-color fluorescent polydopamine nanoprobe for sensing uPA, MMP2, MMP7, and cathepsin B.[23] Algar's group described FRET using semiconductor QDs for the detection of trypsin, chymotrypsin, and enterokinase.[18,19] Besides the above-mentioned general problem with high risk of QDs toxicity, another general disadvantage is their aggregation tendency occurring in the physiological environment and affecting the biomolecule functions.[24] Triple-FRET multi-purpose fluorescent probe for the detection of trypsin, chymotrypsin, and caspase-8 was introduced by our group three years ago.[15] Unfortunately, it can only be used as a "universal single-enzyme" probe to screen three proteases. Although the detection of individual protease pairs was only partially successful, the simultaneous evaluation of all three enzyme species studied in the mixture was unfeasible.

Herein, we study a new multi-purpose FRET peptide probe for the independent and simultaneous detection of more model proteases with the application of only three dyes in various positions in the probe for the detection of individual proteases or their combinations. The system is synthetically very simple and can be easily adjusted to another set of proteases by simply changing the cleavable linker.

Results and discussion

The primary goal of this study is to design and prepare a multi-FRET probe for the detection of three model proteases. Our initial suggestion for the structure of the probe was based on a triple-FRET system with four individual fluorophores. As suitable and readily available dyes, we applied diethylaminocoumarin (DEAC),[25] fluorescein (FL), Rhodamine B (RhB) and HN6.[26] Unfortunately, owing to the failure of several synthetic routes, resulting in the decomposition of the intermediates already modified by FL or HN6 in various combinations of synthetic steps, we were unable to prepare the desired final probe in the appropriate amount and purity. Thus, we decided to replace HN6 with the second molecule of readily available and stable DEAC to obtain a FRET probe (Fig. 1) for the detection of three model enzymes (trypsin, chymotrypsin, and thrombin) as the most common and well available serine proteases.

Probe **1** (Fig. 1) consists of a peptide backbone with three cleavable sites and four fluorophores: two molecules of coumarin (DEAC), fluorescein (FL), and Rhodamine B (RhB). Protease-selective amino acid sequences are linked *via* polyethylene glycol-based (PEG) spacers, allowing the approachability of individual proteases towards their target recognition sites. Upon the excitation of DEAC with a light source of 425 nm, the energy should be transferred through fluorescein (FRET 1a and FRET 1b) to Rhodamine B (FRET 2), resulting in a dominant fluorescence response of Rhodamine B.

After cleavage of a particular peptide sequence by applying a protease, appropriate FRET transfer should be interrupted and a subsequent increase in fluorescence intensity of at least

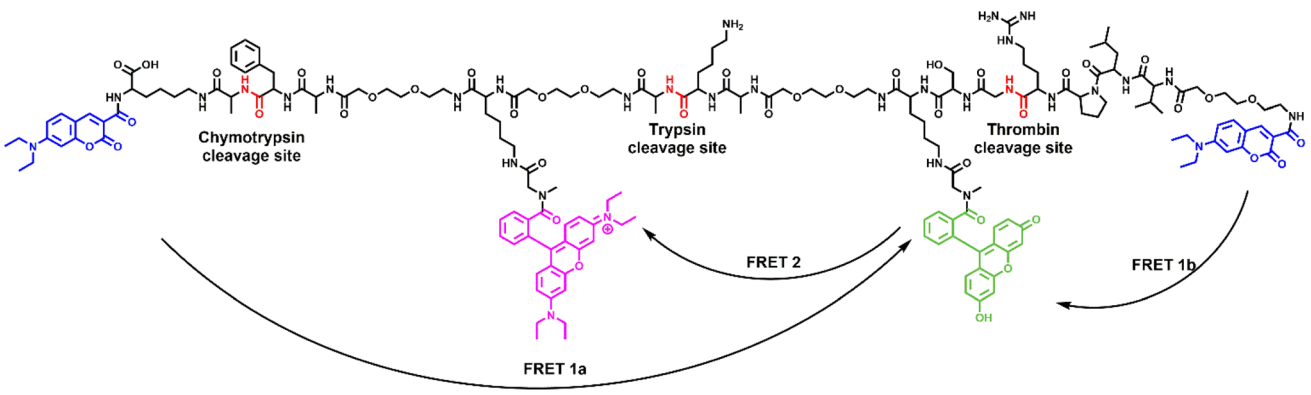

Fig. 1 FRET peptide Probe **1** equipped with coumarin (blue), fluorescein (green) and Rhodamine B (purple).

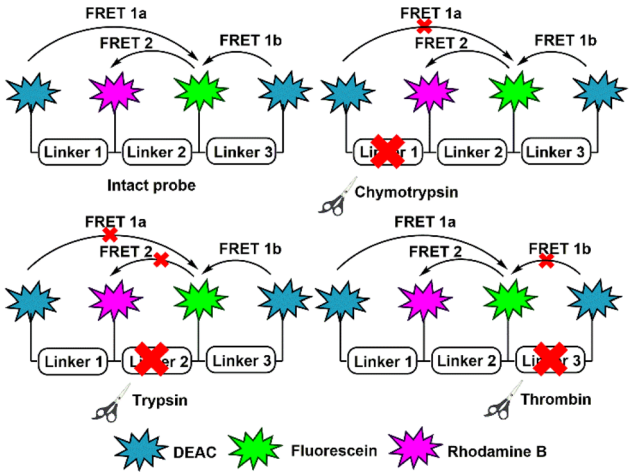

Fig. 2 Suggestion of the basic principle of cleavage mechanism by trypsin, chymotrypsin, and thrombin.

one fluorescent dye should be observed. In the case of chymotrypsin and thrombin linkers, the same donor dyes (DEAC) are used for FRET 1a and 1b, respectively, which indicates the indistinguishability of both enzymes. However, we assumed that the differences in the chemical environment of both peptide-attached DEAC segments, as well as their unequal distances from fluorescein (FRET 1a and 1b acceptors), may result in differences in fluorescence emission profiles and thus enable distinguishing among different combinations of studied proteases. The activities of individual proteases towards peptide Probe **1** are depicted in Fig. 2.

Synthetic approach

Probe **1** (Schemes 1 and S1, SI) was prepared using solid-phase synthesis started by immobilizing Fmoc-Lys(Dde)-OH on Wang resin, followed by the Fmoc deprotection and incorporation of DEAC *via* amide bond as a first fluorophore. After removing Dde from lysine, a peptide backbone was built through a standard Fmoc solid-phase synthesis (Schemes 1 and S1).

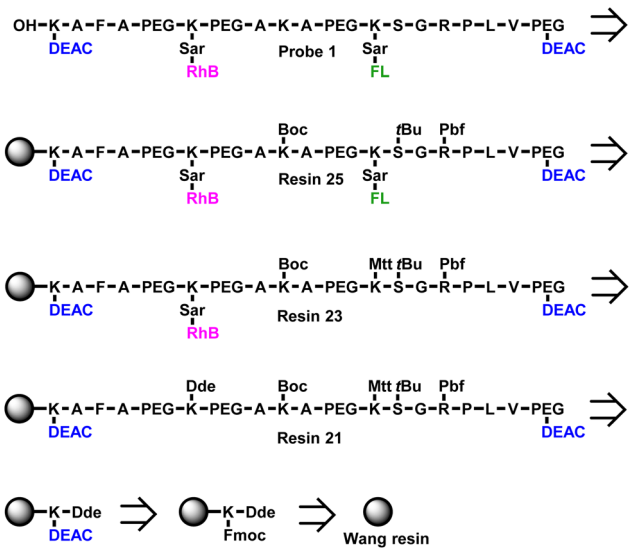

Scheme 1 Retrosynthetic approach to Probe **1**.

The entire synthetic process is depicted in Scheme S1 in the SI.

During this process, three types of Fmoc-protected lysine were used. First, the side chain of Fmoc-Lys(Dde)-OH later served as a binding site for Rhodamine B. Second, Fmoc-Lys(Boc)-OH was utilized as the centre of the trypsin cleavage sequence. Finally, the side chain of Fmoc-Lys(Mtt)-OH was used to immobilize fluorescein. After incorporating a thrombin recognizable site surrounded by two polyethylene glycol spacers, a second molecule of DEAC was attached to afford Resin **21** (Schemes 1 and S1, SI).

In the next step, the protecting group from the lysine moiety placed between the trypsin and chymotrypsin linkers was removed, followed by the attachment of Rhodamine B through the sarcosine scaffold (Resin **23**, Scheme 1). Finally, the Fmoc-Lys(Mtt)-OH moiety located between trypsin and thrombin linker was deprotected and fluorescein was bound to the resin *via* the sarcosine segment to obtain Resin **25** (Scheme 1). Resin **25** was then treated with the cleavage cocktail (50% TFA in DCM) to obtain final peptide Probe **1**. In both cases, sarcosine was used as a source of the tertiary amide of Rhodamine B and fluorescein to avoid the formation of corresponding fluorescence inactive spirolactam scaffolds. Protecting groups on the side chains of amino acids were effectively removed during the treatment of immobilized Resin **25** by cleavage cocktail (50% TFA in DCM). The crude product was purified using a peptide HPLC column (see Material and methods). The desired Probe **1** was isolated with a final purity of approximately 88% (Fig. S6), as apparent from the LC-MS analysis performed on the peptide XB – C18 analytical column.

Spectral properties

Fundamental optical properties of individual fluorescence probes. There are two DEAC molecules attached to the opposite sides of Probe **1**, and their fundamental optical properties were analysed on the synthetically achieved fragments. They are further denoted by ArgDEAC and LysDEAC (Fig. 3). Different modes of attachment resulted in only minor changes in DEAC optical characteristics (Fig. 4). The absorption spectrum of ArgDEAC has its maximum at 430 nm with an extinction coefficient of 42 400 ± 900 M^{-1} cm^{-1}, and the fluorescence emission spectrum has its maximum at 476 nm with a quantum yield of 0.0271 ± 0.0003. The absorption spectrum of LysDEAC has its maximum at 431 nm with an extinction coefficient of 44 200 ± 600 M^{-1} cm^{-1}, and the fluorescence emission spectrum has its maximum at 479 nm with a quantum yield of 0.0237 ± 0.0002.

The properties of fluorescein dye were analysed using the fragment denoted by LysFL (Fig. 3). The absorption spectrum of LysFL has its maximum at 500 nm with an extinction coefficient of 67 000 ± 2000 M^{-1} cm^{-1}, while the fluorescence emission spectrum has its maximum at 521 nm with a quantum yield of 0.775 ± 0.009 (Fig. 4).

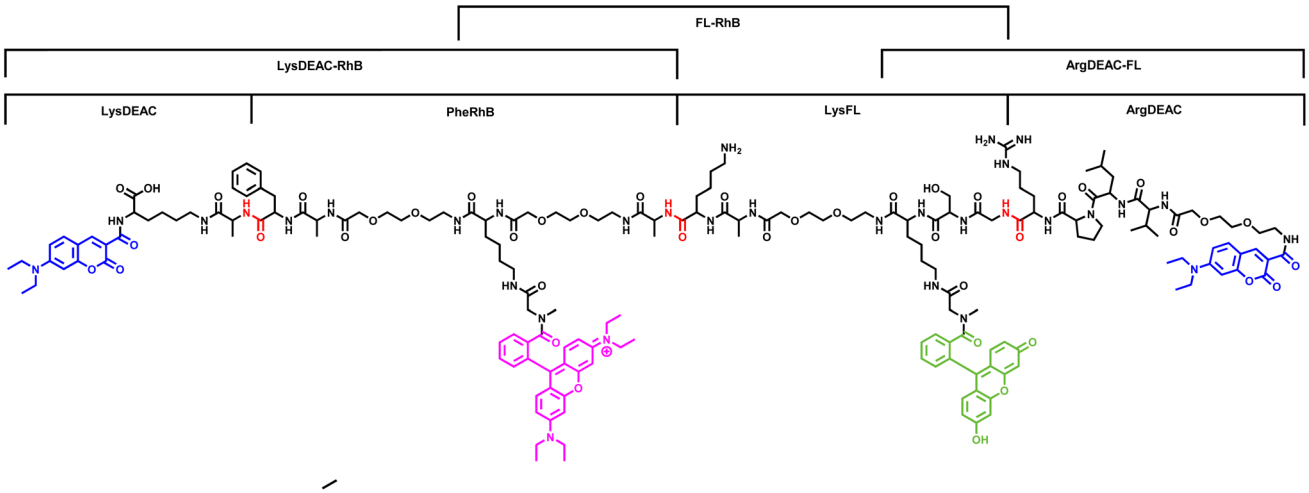

Fig. 3 Structure of Probe **1** and individual fragments used for the determination of optical properties.

The ultimate acceptor in the presumed FRET cascade is the Rhodamine B molecule, and its optical properties were analysed using the fragment denoted by PheRhB (Fig. 3). The absorption spectrum of PheRhB has its maximum at 566 nm with an extinction coefficient of 103 000 ± 4000 M^{-1} cm^{-1}, and the fluorescence emission spectrum has its maximum at 585 nm and a quantum yield of 0.15 ± 0.02 (for excitation at 480 nm) (Fig. 4).

FRET pairs. The absorption and emission spectra described in the previous paragraph were used to calculate the Förster critical distances (R_0) to assess the FRET abilities of each pair of dyes. For the ArgDEAC → LysFL pair, the calculation yielded R_0 = 3.08 ± 0.02 nm. Similarly, for the LysDEAC → LysFL pair, the estimated R_0 value was 3.02 ± 0.02 nm; it was slightly lower owing to the lower quantum yield of LysDEAC compared to ArgDEAC. The largest critical distance was found for the LysFL → PheRhB pair with R_0 = 6.04 ± 0.05 nm, demonstrating excellent spectral overlap, high donor fluorescence quantum yield and high acceptor extinction coefficient. On the contrary, the shortest critical distances were found for the ArgDEAC → PheRhB and LysDEAC → PheRhB pairs with R_0 equal to 2.84 ± 0.02 nm and 2.81 ± 0.02, respectively. Nonetheless, these values indicate that direct energy transfer from DEAC to RhB is possible.

A comparison of the emission spectra of the single-labelled ArgDEAC and LysFL fragments and the double-labelled ArgDEAC-FL construct (Fig. 3) shows the typical behaviour of the FRET pair (Fig. 5). In the double-labelled fragment, the intensity of donor fluorescence decreased, while the acceptor fluorescence was higher compared to the only-acceptor labelled probe. The situation is, however, a little bit more complex in the cases of LysDEAC, PheRhB and double-labelled LysDEAC-RhB fragment (Fig. 3 and 5). Although there is a clear decrease in donor fluorescence, acceptor fluorescence is also decreased in the double-labelled fragment, indicating that interactions other than FRET play a role in this case. The same also holds for LysFL, PheRhB and FL-RhB (Fig. 5). Additionally, in this case, there is a significant decrease in the donor fluorescence in the presence of the acceptor. However, acceptor fluorescence also decreases in the double-labelled construct, indicating the presence of other mechanisms.

Optical properties of Probe 1. The absorption spectrum of Probe **1** is not a simple sum of the absorption spectra of individual dyes (Fig. 4). In the DEAC area, instead of the expected single peak with an extinction coefficient doubled compared to single-labelled DEAC constructs, one can observe a significantly broadened peak with a flat top between 420 and 430 nm. In addition, the fluorescein and Rhodamine B peaks are significantly lower with extinction coefficients of 40 000 ± 2000 M^{-1} cm^{-1} and 42 000 ± 2000 M^{-1} cm^{-1}, respectively, and they are red-shifted to 507 nm and 573 nm, respectively, compared to single-labelled fragments. These observations indicate very strong ground-state interactions. It conflicts with the axioms of FRET theory assuming excited-state energy transfer as the only interaction between donor and acceptor. Thus, the precise calculation of the FRET efficiencies of distances between dyes in terms of FRET theory is meaningless.

Fortunately, it does not compromise Probe **1** from being used as a fluorescence sensor for monitoring enzyme activities. Upon excitation at 421 nm (DEAC), the fluorescence quantum yield is 0.00542 ± 0.00003, and we observe that the fluorescence intensity of Probe **1** is approximately 50-fold lower at 476 nm (DEAC) than that of ArgDEAC, approximately 16-fold lower at 521 nm (FL) than that of LysFL and approximately 2.3-fold lower at 585 nm (RhB) than that of PheRhB. Similarly, upon excitation at 480 nm (FL), the fluorescence quantum yield is 0.0111 ± 0.0006, and there is approximately 200-fold lower Probe **1** fluorescence at 521 nm (FL) than that of LysFL or approximately 8-fold lower at 585 nm (RhB) than that of PheRhB. These changes can be used to monitor enzyme activities.

Mono-enzyme assays. To evaluate whether the presented probe can monitor enzyme activities, the probe's responses towards individual proteases (trypsin, chymotrypsin and thrombin) were examined. For this purpose, it was necessary to

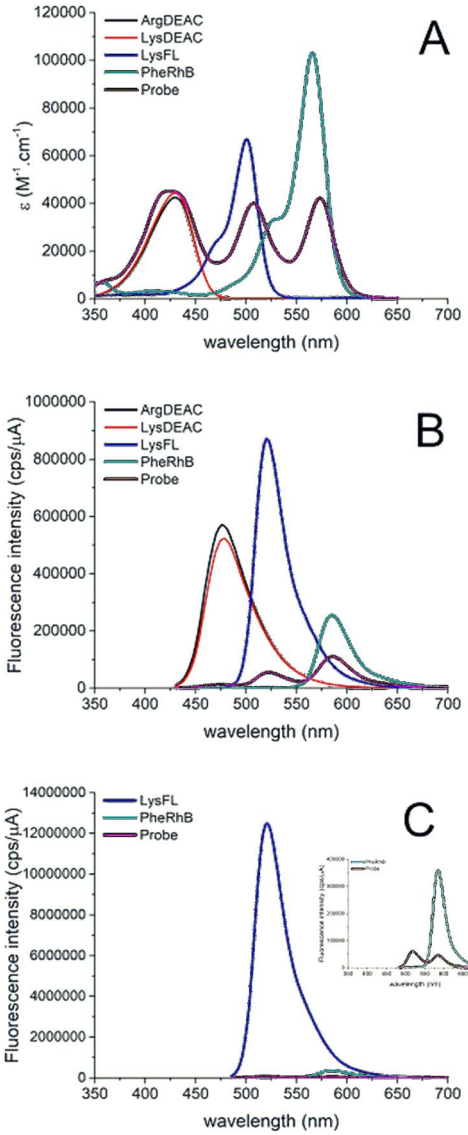

Fig. 4 Absorption spectra (A), fluorescence emission spectra on excitation at 421 nm (B) and fluorescence emission spectra on excitation at 480 nm (C) of ArgDEAC, LysDEAC, LysFL, PheRhB and Probe **1**. Inset: magnified spectra of PheRhB and Probe **1**. Spectra of ArgDEAC, LysDEAC and the Probe **1** were measured at 1 μM concentration, while the spectra of LysFL and PheRhB were measured at 0.5 μM concentration. Therefore, for easier comparison, the fluorescence spectra of LysFL and PheRhB are displayed after multiplication by a factor of 2.

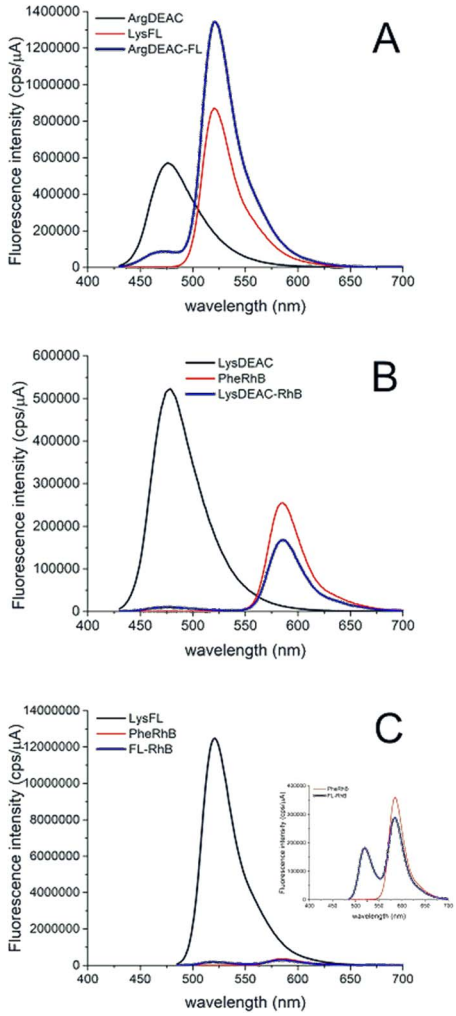

Fig. 5 Fluorescence emission spectra of the donor (black), acceptor (red) and donor–acceptor pair (blue): (A) ArgDEAC, LysFL and ArgDEAC-FL, respectively; (B) LysDEAC, PheRhB and LysDEAC-RhB, respectively; and (C) LysFL, PheRhB and FL-RhB, respectively. Inset: magnified spectra of PheRhB and Probe **1**. Spectra of ArgDEAC, LysDEAC, ArgDEAC-FL and LysDEAC-RhB were measured at 1 μM concentration, while the spectra of LysFL, PheRhB and FL-RhB were measured at 0.5 μM concentration. Therefore, for easier comparison, the fluorescence spectra of LysFL, PheRhB and FL-RhB are displayed after multiplication by a factor of 2.

begin with the confirmation of the photostability of Probe **1** under the conditions of enzymatic cleavage. With this aim, intact Probe **1** was dissolved in Tris buffer and incubated at 37 °C. After measuring fluorescence emission at t_0, 1 mM HCl (serving as a medium for reconstituting trypsin and chymotrypsin) or physiological saline solution (serving as a medium for reconstituting thrombin) was added. Fluorescence emission responses of all fluorophores were then monitored for 75 minutes upon excitation at 425 nm. As illustrated in Fig. 6, the fluorescence intensities of individual dyes remained nearly

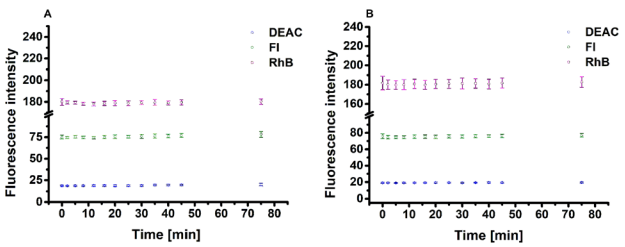

Fig. 6 Fluorescence emission responses of Probe **1** over time in the presence of 1 mM HCl (A) and physiological solution (B) in Tris buffer (pH = 8.0). λ_{EXC} = 425 nm, λ_{EMS} = 475 nm (DEAC); 526 nm (FL) and 590 nm (RhB). Each measurement was carried out in triplicate. The average values and standard deviations (n = 3) were calculated and graphically presented.

unchanged during the experimental period, confirming the sufficient stability of Probe **1** in the buffer solution.

In the next step, the cleavability of Probe **1** by individual proteases was studied, followed by determining the lowest detectable concentrations of individual enzymes. Starting with trypsin, an expected increase in fluorescein emission as a result of the cleavage of the peptide linker between the N-terminus of alanine and the C-terminus of lysine (Fig. 1) was observed. In addition, an increase in DEAC emission was detected (Fig. 7A).

LC-MS analysis of Probe **1** after trypsin cleavage showed the formation of expected fragments after the hydrolysis of the trypsin linker, but fragments corresponding to hydrolysis of the Arg–Gly peptide bond in the thrombin recognition site, explaining the detected increase in DEAC fluorescence response (Fig. S15 in SI). The observed emission trend was reproducible until a trypsin concentration of 0.0625 ng mL^{-1}, causing an increase in fluorescein emission of 24% over 75 min (Fig. S19, SI). With two times (0.125 ng mL^{-1}), four times (0.25 ng mL^{-1}), eight times (0.5 ng mL^{-1}) and sixteen times (1 ng mL^{-1}) higher concentrations of trypsin in a sample, the increases in FL and DEAC emission responses were more evident (Fig. 7A and S16–S19, SI).

In the case of chymotrypsin, a noticeable increase in DEAC fluorescence response (by 55% during 75 minutes) corresponding to cleavage between the N-terminus of Ala and C-terminus of Phe was observable until the concentration of 0.125 μg mL^{-1} (Fig. 7B). In addition, we observed a slight elevation of fluorescein emission, which was remarkable, especially at higher concentrations of chymotrypsin in solution (2 μg mL^{-1}, 1 μg mL^{-1}, 0.5 μg mL^{-1} and 0.25 μg mL^{-1} (Fig. S21–S24, SI)). LC-MS analysis of Probe **1** after chymotrypsin treatment confirmed the formation of the expected fragments obtained by hydrolysis of the trypsin linker in a minority and thrombin linker, similar to trypsin cleavage (Fig. S20 in SI).

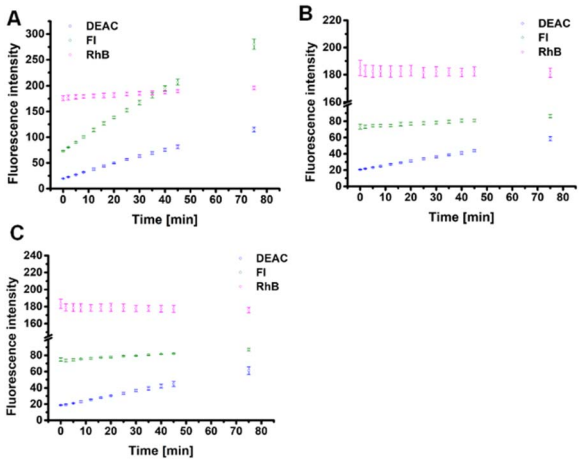

Fig. 7 Fluorescence emission responses of Probe **1** (c = 0.01 mM) over time in the presence of (A) trypsin (c = 1 ng mL^{-1}), (B) chymotrypsin (c = 0.125 μg mL^{-1}) and (C) thrombin (c = 0.0125 U mL^{-1}). λ_{EXC} = 425 nm, λ_{EMS} = 475 nm, 526 nm, and 590 nm (DEAC, FL, and RhB). Each measurement was carried out in triplicate. The average values and standard deviations (n = 3) were calculated, and they are graphically presented.

Finally, the characteristic emission pattern of thrombin was examined. Based on an increase in DEAC emission, we were able to detect thrombin until a concentration of 0.78 mU mL^{-1}. However, the reproducibility was unsatisfactory. Thus, its lowest detectable concentration was finally estimated to be 0.0125 U mL^{-1} (Fig. 7C). The observed trend was confirmed by the treatment of Probe **1** with four higher concentrations (0.2 U mL^{-1}, 0.1 U mL^{-1}, 0.05 U mL^{-1} and 0.025 U mL^{-1}) of thrombin (Fig. S26–S29, SI).

In line with the methodology used in previous studies,[12,14] the activity of all three proteases can be graphically presented by a ratiometric graphical model using the ratios of the fluorescence emission responses of individual fluorophores (Table 1) measured at particular times. The ratio of fluorescence response change in DEAC (λ_{EMS} = 475 nm) and FL (λ_{EMS} = 526 nm) within an appropriate time was designated as X (X = DEAC(I_t/I_0)/FL(I_t/I_0)). A similar ratio of fluorescence response change in RhB (λ_{EMS} = 590 nm) and DEAC (λ_{EMS} = 475 nm) within the same period was designated as Y (Y = RhB(I_t/I_0)/DEAC(I_t/I_0)) and ratio of the fluorescence response change in RhB (λ_{EM} = 590 nm) and FL (λ_{EM} = 526 nm) was designated as Z (Z = RhB(I_t/I_0)/FL(I_t/I_0)) (Table 1).

For the mono-enzyme assay, values of X and Y obtained within 75 minutes were plotted to X–Y coordinates (Fig. 8). It is evident that the presence of individual proteases could be depicted with their characteristic curves. However, the curve of thrombin partially overlaps with the curve of chymotrypsin. It was necessary to find a rule to distinguish the co-presence of these two enzymes. As depicted in Fig. S26–S29 (SI), thrombin can also be characterized by a decrease in the fluorescence response of RhB (detectable at a concentration of 0.025 U mL^{-1} and higher) in contrast to chymotrypsin, with RhB emission intensity nearly constant (Fig. 7B and S21–S24, SI). By combining a graphical model and the RhB fluorescence response, we can determine the presence of an appropriate protease in a monoenzymatic sample.

Double enzyme assay. After the successful development of the methodology for the detection of a single protease, we decided to investigate the possibilities of the simultaneous detection of multiple enzymes. In the double-enzyme assay, all three possible pairs of appropriate proteases at the combinations of their maximal and minimal concentrations determined in the previously described single-enzyme assay were studied. As discussed above, each protease at various concentrations, if present as a single one, can be identified according to its

Table 1 Definition of ratios used in graphical models[a]

Ratio	Fluorophores
X	$(I_t/I_0)_{EMS475}/(I_t/I_0)_{EMS526}$
Y	$(I_t/I_0)_{EMS590}/(I_t/I_0)_{EMS475}$
Z	$(I_t/I_0)_{EMS590}/(I_t/I_0)_{EMS526}$

[a] EMS_{475}, EMS_{526} and EMS_{590} belong to the fluorescence emission of DEAC, FL and RhB, respectively. I_t and I_0 represent intensities of fluorescence at appropriate time "t" of cleavage and time "0", respectively.

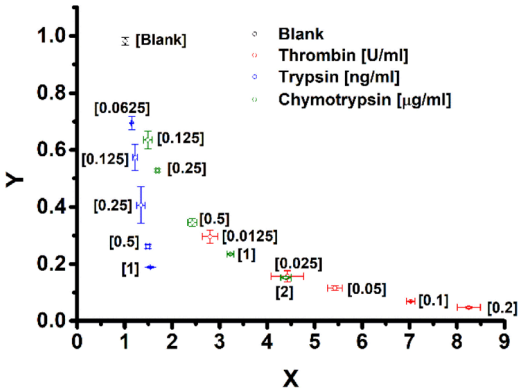

Fig. 8 Graphical visualization of individual protease detection. Variables X and Y represent the ratios of fluorescence emission responses for appropriate fluorophores measured at 75 min (I_{75min}) and 0 min (I_{0min}) ($n = 3$), respectively, and they are defined in Table 1.

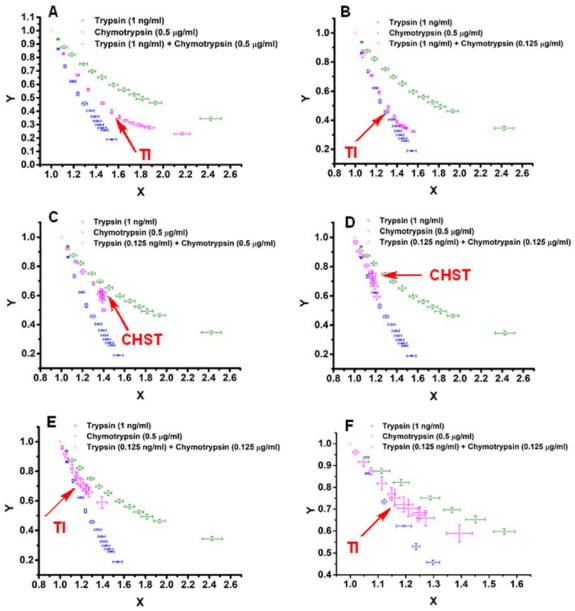

Fig. 9 Fluorescence emission responses of Probe **1** over time in the presence of trypsin (low concentration (lowTRYP): 0.125 ng mL^{-1}; high concentration (high(TRYP): 1 ng mL^{-1}), chymotrypsin (low concentration (lowCHYM): 0.125 μg mL^{-1}; high concentration (highCHYM): 0.5 μg mL^{-1}), and appropriate inhibitor: (A) highTRYP–highCHYM and trypsin inhibitor (TI), 10 ng mL^{-1}; (B) highTRYP–lowCHYM and trypsin inhibitor (TI), 10 ng mL^{-1}; (C) lowTRYP–highCHYM and chymotrypsin inhibitor (CHST), 60 μg mL^{-1}; (D) lowTRYP–lowCHYM and chymotrypsin inhibitor (CHST), 60 μg mL^{-1}; (E) lowTRYP–lowCHYM and trypsin inhibitor (TI), 10 ng mL^{-1}; and (F) detail of (E). The measurements were performed in Tris buffer (pH = 8.0) at 37 °C. After 16 min of monitoring, the inhibitor was added. Each measurement was carried out in triplicate. The average values and standard deviations ($n = 3$) were calculated and are graphically presented.

characteristic curve in the graphical model (Fig. 8) and RhB fluorescence response (Fig. 7B and S21–S24 and S26–S29, SI). In the case of the two enzymes used in the assay, the tentative results show that the position of the curve depends on the type of enzymes and their concentrations, and it is often identical to the lines of single enzymes. Thus, to clearly identify the composition of the enzymatic solution, the use of the graphical model presented in Fig. 8 as the only tool is insufficient. Therefore, we decided to apply selective inhibitors as a contributing factor, which should cause a change in the appropriate curve trend. Experimentally, the assay had to be slightly modified by the addition of an appropriate inhibitor after 16 minutes (when the curves were sufficiently apart from each other to observe the change in their trends) of incubation, resulting in the immediate deactivation of one protease, whereas the second one remained active.

Starting with a pair of trypsin and chymotrypsin, Kunitz trypsin selective inhibitor (TI) and chymostatin (CHST) as a selective chymotrypsin inhibitor were studied. After the addition of enzymes to the solution of Probe **1** in Tris buffer, the progress of the experiment was monitored over time using the ratiometric model and compared with the curve of trypsin and chymotrypsin when solely present (Fig. 8) to distinguish which inhibitor should be used. In general, at high concentrations of trypsin and low concentrations of chymotrypsin, the assay curve was very similar to the trypsin line; therefore, a trypsin inhibitor was added after 16 minutes. After that, we can observe a significant break and change in the direction of the curve towards the chymotrypsin one (Fig. 9B). In the case of low trypsin concentrations and high chymotrypsin concentrations, the curve closely resembled the characteristic of chymotrypsin only; therefore, the inhibitor of chymotrypsin was used, resulting in a break of the curve towards trypsin one (Fig. 9C). When trypsin and chymotrypsin are presented in low concentrations, the position of the curve is located between the curves of individual enzymes. It is evident from Fig. 9D–F that any of the inhibitors can be used in this case, resulting in a change in direction towards the non-inhibited enzyme. Using the described methodology, we can detect trypsin at concentrations of 0.125 ng mL^{-1} and higher (verified up to 1 ng mL^{-1}) and chymotrypsin in a verified concentration range of 0.125–0.5 μg mL^{-1} in their mixture. It is clear that this assay is suitable for all three scenarios characteristic of two enzyme detection; each protease is present as the single enzyme, or both proteases are present in the sample because the curve does not continue after inhibitor addition if the single enzyme is present.

Similarly, the same methodology was applied to the trypsin/thrombin pair. For this purpose, the Kunitz trypsin inhibitor was used in all experiments. Owing to the dominant response of thrombin on the above-mentioned graphical model in Fig. 8, which was independent of the amount of trypsin in the sample, we were not able to observe remarkable changes after trypsin inhibition (Fig. S30, SI). Thus, the ratio of RhB/DEAC (Y) plotted on the Y axis was replaced by monitoring the RhB/FL ratio (Z) (Table 1). In this model, linear curves for trypsin and thrombin can be observed, and the curve corresponding to the mixture of these two enzymes is located between them (Fig. 10). Inhibition of trypsin after 16 minutes of the assay results in a break and changes in linearity towards the thrombin line (Fig. 10). The detection of trypsin (0.5 ng mL^{-1}–1 ng mL^{-1}) in a mixture with thrombin (0.0125–0.2 U mL^{-1}) was verified by applying this method.

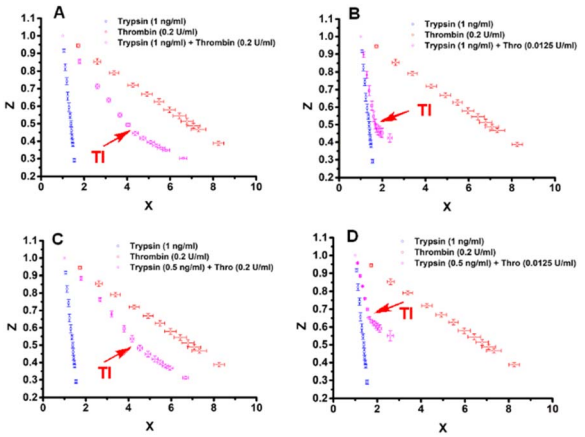

Fig. 10 Fluorescence emission responses of Probe 1 over time in the co-presence of trypsin (low: 0.5 ng mL^{-1}; high: 1 ng mL^{-1}), thrombin (low: 0.0125 U mL^{-1}; high: 0.2 U mL^{-1}) and trypsin inhibitor (TI) 10 ng mL^{-1}: (A) highTRYP–highTHROM, (B) highTRYP–lowTHROM, (C) lowTRYP–highTHROM, and (D) lowTRYP–lowTHROM. The measurements were performed in Tris buffer (pH = 8.0) at 37 °C. After 16 min of monitoring, the inhibitor was added. Each measurement was carried out in triplicate. The average values and standard deviations were calculated (n = 3) and graphically presented.

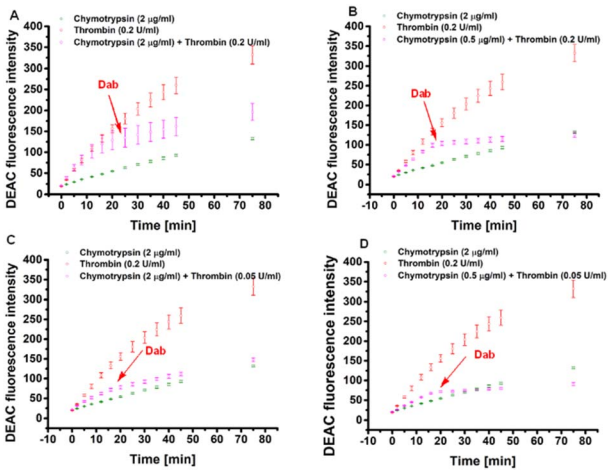

Fig. 11 Fluorescence emission responses of Probe 1 over time in the co-presence of chymotrypsin (low: 0.5 μg mL^{-1}; high: 2 μg mL^{-1}), thrombin (low: 0.05 U mL^{-1}; high: 0.2 U mL^{-1}) and thrombin inhibitor (Dab) 0.5 μg mL^{-1}: (A) highCHYM–highTHROM, (B) lowCHYM–highTHROM, (C) highCHYM–lowTHROM, and (D) lowCHYM–lowTHROM. The measurements were performed in Tris buffer (pH = 8.0) at 37 °C. After 16 min of monitoring, the inhibitor was added. Each measurement was carried out in triplicate. The average values and standard deviations (n = 3) were calculated and are graphically presented.

Finally, the enzyme activities of the chymotrypsin/thrombin pair were examined. Initially, the chymotrypsin inhibitor was used in combination with a graphical ratiometric model using X–Y coordinates. Unfortunately, probably owing to a similar characteristic pattern of chymotrypsin and thrombin (Fig. 8), no significant change was observed after the addition of the inhibitor. Similar results were also obtained by inhibiting thrombin with its selective inhibitor dabigatran. Instead of the above-mentioned developed graphical ratiometric model, the dependence of DEAC fluorescence emission on time was found to be a useful tool for chymotrypsin/thrombin recognition. As shown in Fig. 11, the inhibition of thrombin after 16 minutes results in a change in the direction of the monitored curve, which becomes linear, similar to the line characteristic for chymotrypsin. By applying this approach, we were able to detect chymotrypsin in a concentration range of 0.5–2 μg mL^{-1} in the mixture with thrombin at a concentration range of 0.05–0.2 U mL^{-1} at the cost of losing the advantage of ratiometric measurement.

Triple enzyme assay. Finally, we tried to develop a methodology for the simultaneous detection of all three proteases in different concentration combinations. For this purpose, we designed an assay with the sequential use of various combinations of the two inhibitors. The first inhibitor was added after 16 minutes of assay, and we expected to observe a change in the curve direction, indicating the inhibition of the first enzyme. The second inhibitor was added after 60 minutes of the experiment with the expectation of another change in the curve direction, confirming the inhibition of the second enzyme. The assay was then continued for another 60 minutes to observe the progress of the curve related to the third enzyme.

The individual combinations of inhibitors were examined in an effort to find a uniform method. Proteases were combined at their low and high concentrations, resulting from a double-enzyme assay: trypsin (low: 0.5 ng mL^{-1}; high: 1 ng mL^{-1}), chymotrypsin (low: 0.5 μg mL^{-1}; high: 2 μg mL^{-1}), and thrombin (low: 0.05 U mL^{-1}; high: 0.2 U mL^{-1}). The obtained data were evaluated on a graphical model using variables X and Z (Table 1) plotted to X and Y coordinates, respectively.

First, the combination of a trypsin inhibitor, followed by chymostatin, was examined in mixtures of proteases with a high concentration of trypsin (1 ng mL^{-1}) and various concentrations of the other two enzymes. In all cases, the addition of trypsin inhibitor resulted in a break in the curve, confirming the presence of trypsin in the sample, as illustrated in Fig. 12A. Unfortunately, the subsequent addition of chymostatin did not result in an expected change in the plot (Fig. 12A). Thus, it was not possible to distinguish between chymotrypsin and thrombin in the sample. Therefore, chymostatin was replaced with the thrombin inhibitor dabigatran and used with the same as well as the other enzyme concentration combinations. In a few examples (even at high concentrations of all enzymes or at low concentrations of chymotrypsin and thrombin), we detected trypsin after the addition of trypsin inhibitor (see example in Fig. 12B), but the addition of dabigatran did not help with the determination of the other two enzymes because the curve did not change anymore.

After that, the use of dabigatran, followed by chymostatin, was examined. In this case, the observable changes in the plot after individual inhibitions were observed only in one example regarding trypsin and thrombin at high concentrations with a mixture of low chymotrypsin concentrations (Fig. 12C; detail in Fig. S31, SI).

Finally, the combination of chymostatin as the first inhibitor, followed by the inhibition of trypsin, turned out to be the

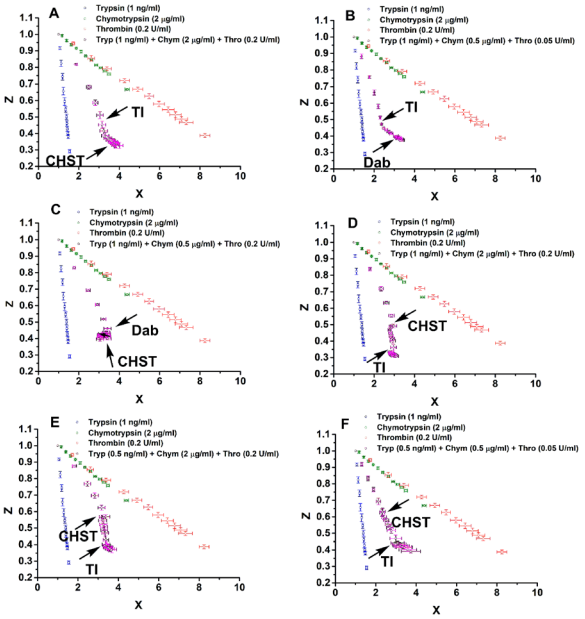

Fig. 12 Fluorescence emission responses of Probe **1** over time in the co-presence of trypsin (low: 0,5 ng mL^{-1}; high: 1 ng mL^{-1}), chymotrypsin (low: 0.5 μg mL^{-1}; high: 2 μg mL^{-1}), thrombin (low: 0.05 U mL^{-1}; high: 0.2 U mL^{-1}) and trypsin inhibitor (TI), chymotrypsin inhibitor (CHST) and thrombin inhibitor (DAB): (A) highTRYP–highCHYM–highTHROM, (B) highTRYP–lowCHYM–lowTHROM, (C) highTRYP–lowCHYM–highTHROM, (D) highTRYP–highCHYM–highTHROM, (E) lowTRYP–highCHYM–highTHROM, and (F) lowTRYP–lowCHYM–lowTHROM. The measurements were performed in Tris buffer (pH = 8.0), at 37 °C. Each measurement was carried out in triplicate. The average values and standard deviations (n = 3) were calculated and are graphically presented.

most promising. In more than half of the examples, after inhibition, we were able to observe changes in the direction of tracking assay lines, confirming the presence of chymotrypsin, trypsin and thrombin, as depicted in Fig. 12D and E. In two cases, it was not possible to confirm the presence of chymotrypsin, but the break and continuation of the assay after the second inhibition indicated the presence of trypsin and thrombin in the studied solution (Fig. 12F and S32, SI). In one example (trypsin and thrombin at high concentrations and low chymotrypsin concentrations), the shape of the curve remained nearly unchanged; thus, it was impossible to distinguish among individual enzymes at this concentration combination (Fig. S33).

Experimental

Materials and methods

Peptide Probe **1** (Fig. 1) was synthesized on commercially available Wang resin (0.9 mmol g^{-1}, AAPPTec, Louisville, KY, USA) using multi-step peptide solid-phase synthesis. The chemicals and solvents were obtained from the available commercial sources; 7-(diethylamino)coumarin-3-carboxylic acid (DEAC) was synthesized according to the described procedure.[25]

Synthesis, isolation and storage

Solid-phase synthesis was performed in plastic reaction vessels (syringes equipped with one porous disk each) using a manually operated synthesizer.[27] The volume of the wash solvent was 10 mL per gram of the resin. For washing, the slurry was shaken 5× with fresh solvent for at least 1 min before the solvent was replaced. The synthetic scheme with specific reaction conditions is depicted in (SI – Scheme 1).

To analyse an intermediate after each reaction step, a small amount of resin-bound peptide was treated with 50% TFA in DCM to perform chemical cleavage from a solid support. Volatiles were evaporated by the gentle stream of nitrogen, and the residuum was dissolved in acetonitrile/water 1 : 1 (v/v) and analysed on a UHPLC chromatograph (Acquity) using a photodiode array detector and a single quadrupole mass spectrometer (Waters, Borehamwood, UK), employing C-18 Xselect HSS T3 2.5 μm XP (50 × 3.0 mm) column (Waters, Borehamwood, UK). As the mobile phase, ammonium acetate (10 mM) in ultrapure water and acetonitrile (gradient 20–80% over the first 4.5 min) or 0.1% HCOOH in ultrapure water (v/v) and acetonitrile (gradient 20–80% over the first 4.5 min) were used. The purity of the compounds was determined as the ratio of the given peak area to the total area of all peaks of the mixture.

For isolation, the resin-immobilized final crude product was treated with 50% TFA in DCM for 60 min. Then, the volatiles were removed under a stream of nitrogen. Oily residuum was dissolved in acetonitrile/water 1 : 1, and purification was performed on a semi-prep HPLC column (Aeris 5 μm 150 × 21.2 mm peptide XB-C18 100 Å, Phenomenex, California, USA) using a gradient of 50–80% acetonitrile in 0.1% TFA in ultrapure H_2O within 10 min. The combined fractions were concentrated *in vacuo* and freeze-dried for 48 hours (Scanvac Coolsafe Freeze Dryer, LaboGene, Lillerød, Denmark) to obtain a dark red powder that was afterwards stored at −80 °C in a deep freezer (Arctiko, Esbjerg Kommune, Denmark).

Compound characterization

Isolated Probe **1** was characterized by LC-MS analysis and HRMS. HRMS analysis was performed on an LC chromatograph Dionex UltiMate 3000 (Thermo Fischer Scientific, MA, USA) equipped with an Exactive Plus Orbitrap high-resolution mass spectrometer (Thermo Fischer Scientific, MA, USA) operating in positive and negative full scan modes in the range of 2000–3000 m/z. Final purity was determined based on the LC-MS analysis of a peptide column (150 × 4.6 mm bioZen 2.6 μm peptide XB-C18, Phenomenex, USA).

Absorption spectra

Absorption spectra of 1 μM (LysDEAC, ArgDEAC, DEAC-FL, DEAC-RhB, and Probe **1**) or 0.5 μM (LysFL, PheRhB, and FL-RhB) solutions in 0.1 M Tris–HCl, pH = 8.0, were recorded using an SP-UV1100 spectrometer (DLAB Scientific) in a PMMA cuvette with a 1 cm optical path, using a pure solvent as a reference. The spectra were measured in the 350–650 nm

interval with a 1 nm step. The extinction coefficient $\varepsilon(\lambda)$ was calculated using formula (1):

$$\varepsilon(\lambda) = \frac{A(\lambda)}{cl}, \quad (1)$$

where $A(\lambda)$ is the estimated absorbance, c is the sample concentration, and l is the optical path. All samples were measured in 5–10 replicates.

Steady-state fluorescence spectra

The steady-state emission spectra of the solutions described in the previous paragraph were recorded using a Fluorolog-3 fluorometer (Jobin-Yvon, France). The absorbance of the sample at the excitation wavelength should be below 0.05 in all cases; therefore, the inner-filter effect could be neglected. Emission spectra for direct DEAC excitation were recorded using an excitation monochromator at 421 nm, while for direct fluorescein excitation, the excitation monochromator was set to 480 nm. In all cases, bandpasses in both the excitation and emission monochromators were set to 2 nm, and the spectra were scanned with 1 nm steps and an integration time of 0.2 s per data point at 22 °C (Peltier controlled).

Quantum yield (QY) estimation

Emission spectra were obtained under the conditions described above. For spectra obtained with excitation at 421 nm, a solution of 0.5 μM coumarin 153 in ethanol was used as a quantum yield standard (QY = 0.38),[28] and the fluorescence intensity was integrated in the 430–700 nm interval, while for spectra obtained with excitation at 480 nm, a solution of 0.05 μM fluorescein in 0.1 M NaOH was used as a quantum yield standard (QY = 0.95),[29] and the fluorescence intensity was integrated in the 485–700 nm interval. The quantum yield (QY) was calculated using eqn (2):

$$\mathrm{QY} = \frac{\varepsilon_S}{\varepsilon}\frac{F}{F_S}\frac{n^2}{{n_S}^2}\mathrm{QY}_S, \quad (2)$$

where ε, F and n denote the extinction coefficient at the excitation wavelength, integrated fluorescence intensity and refractive index, respectively, and the subscript "S" denotes the standard. All samples were measured in five replicates.

Determination of the Förster distance R_0

Förster distance was calculated from the spectral properties of the donor and the acceptor and the donor quantum yields using eqn (3):

$${R_0}^6 = \frac{9000(\ln 10)\kappa^2 Q_D}{128\pi^5 N_{Av} n^4}\int_0^\infty F_D(\lambda)\varepsilon_A(\lambda)\lambda^4 d\lambda, \quad (3)$$

where Q_D is the quantum yield of the donor in the absence of acceptor, n is the refractive index of the medium, N_{Av} is Avogadro's number, $F_D(\lambda)$ is the normalized fluorescence intensity of the donor, $\varepsilon_A(\lambda)$ is the extinction coefficient of the acceptor, and κ^2 is a factor describing the relative orientation in the space of the transition dipoles of the donor and acceptor. We considered a random orientation of dipoles, which yields $\kappa^2 = 2/3$.

Proteases, inhibitors and buffer solutions

Trypsin (bovine pancreas, TPCK treated, ≥10 000 BAEE units per mg protein), α-chymotrypsin (bovine pancreas, TLCK treated, type VII, ≥40 units per mg protein), and thrombin (bovine plasma, ≥60 units per mg protein) were ordered from Sigma-Aldrich (Steinheim, Germany). All enzyme species were obtained as lyophilized white powders. They were reconstituted according to the providers' instructions, aliquoted in Eppendorf tubes, and stored at −80 °C in a deep freezer (Arctiko, Esbjerg Kommune, Denmark). Trypsin inhibitor (*Glycine max*) and chymostatin were purchased from Merck (Darmstadt, Germany). Dabigatran was purchased from BLD Pharmatech (Reinbek, Germany). Enzyme assays were carried out in 0.1 M Tris buffer solution in ultrapure water; the pH of the media (pH = 8.0) was adjusted by gradual dropwise addition of a concentrated NaOH aqueous solution.

Single protease detection

10 μL of FRET peptide probe solution in DMSO (0.5 mM) was added to 480 μL of Tris buffer. The resulting solution was placed into a polystyrene fluorescence cuvette and preheated to 37 °C. Afterwards, the fluorescence emission spectrum upon excitation with a light source of 425 nm was measured at 0 min using a fluorescence spectrometer (Cary Eclipse, Agilent Technologies, Santa Carla, CA, USA). Then, 10 μL of 1 mM HCl with/without enzyme (trypsin or chymotrypsin) or 10 μL of physiological saline solution with/without enzyme (thrombin) was added, resulting in a final volume of 500 μL of 0.01 mM Probe **1**. Fluorescence emission responses were then repeatedly measured at the times 2, 5, 8, 12, 16, 20, 25, 30, 35, 40, 45 and 75 min. During the entire period of the experiment, a fluorimeter cuvette was placed in a cell holder preheated to 37 °C and located inside a fluorescence spectrometer.

Simultaneous screening of two proteases

10 μL of FRET peptide probe solution in DMSO (0.5 mM) was added to 470 μL of Tris buffer. The resulting solution was placed into a polystyrene fluorescence cuvette and preheated to 37 °C. Afterwards, the fluorescence emission spectrum upon excitation with a light source of 425 nm was measured at 0 min using a fluorescence spectrometer (Cary Eclipse, Agilent Technologies, Santa Carla, CA, USA). Then, 10 μL of each enzyme in the appropriate solvent (1 mM HCl for trypsin or chymotrypsin and physiological saline solution for thrombin) was added. Fluorescence emission responses were then measured at 2, 5, 8, 12, and 16 min, followed by the addition of 10 μL of an appropriate inhibitor (Trypsin inhibitor 500 ng mL^{-1} in Tris buffer; Chymostatin 3 mg mL^{-1} in DMSO; Dabigatran 25 μg mL^{-1} in Tris buffer). Fluorescence response was then measured at 20, 25, 30, 35, 40, 45 and 75 min.

Simultaneous screening of three proteases

10 μL of FRET peptide probe solution in DMSO (0.5 mM) was added to 460 μL of Tris buffer. The resulting solution was placed into a polystyrene fluorescence cuvette and preheated to 37 °C.

Afterwards, the fluorescence emission spectrum upon excitation with a light source of 425 nm was measured at 0 s using a fluorescence spectrometer (Cary Eclipse, Agilent Technologies, Santa Carla, CA, USA). Then, 10 μL of each enzyme in the appropriate solvent (1 mM HCl for trypsin or chymotrypsin and physiological saline solution for thrombin) was added. Fluorescence emission responses were then measured at 2, 5, 8, 12, and 16 min, followed by the addition of 10 μL of an appropriate inhibitor (Trypsin inhibitor 500 ng mL^{-1} in Tris buffer; chymostatin 3 mg mL^{-1} in DMSO; Dabigatran 25 μg mL^{-1} in Tris buffer). The fluorescence response was then measured at 20, 25, 30, 35, 40, 45 and 60 min. After that, 10 μL of the second inhibitor was added (Trypsin inhibitor 500 ng mL^{-1} in Tris buffer; chymostatin 3 mg mL^{-1} in DMSO; 25 μg mL^{-1} in Tris buffer), followed by measuring fluorescence response at 65, 70, 75, 80, 85, 90, 105 and 120 min.

Conclusions

In summary, a multi-purpose FRET peptide fluorescent probe was synthesized using multistep solid-phase synthesis. The investigation of the probe's optical properties revealed significant ground-state interactions, indicating that alongside FRET, additional mechanisms also influence its optical behaviour. The prepared probe was then studied as a suitable tool for the simultaneous detection of trypsin, chymotrypsin and thrombin even as an individual enzyme or in two-enzyme or three-enzyme mixtures. In a single-enzyme mode, we can clearly distinguish which enzyme is present using a ratiometric graphical model (Fig. 7 and 8). The probe can be used as a general tool for identifying one protease in a mixture or a mixture of two proteases. An unambiguous detection model for all these scenarios has been developed. In the case of two-enzyme mixtures, we developed an assay using selective inhibitors and real-time monitoring of enzymatic cleavage, which allowed us to simultaneously detect individual proteases in each pair (Fig. 9–11). Finally, the screening of a three-enzyme mixture was examined using a graphical model and a combination of two selective inhibitors. Although different combinations of inhibitors were tested (see examples in Fig. 12), none of them was shown to be universal for the detection of all three enzymes together.

Although the data indicate that FRET is not the only mechanism responsible for the observed changes in fluorescence intensity at various wavelengths, the probe successfully reflects the presence of enzymes alone or in various dual combinations, unfortunately, except for all three proteases present together. The presented probe is, thus, representative of a universal tool for the detection of three proteases as individual species or their couples in various combinations. Probe **1** was developed as a model probe. The probe can be easily modified by changing individual recognition sites to any other protease; of course, the detection limits must be determined individually for such a probe. The resulting fluorophore emission patterns after cleavage of specific linkers should be completely independent of the enzymes used. Despite the limitations discussed above, the developed method of probe preparation, together with inexpensive instrumentation, common reaction methodology and simple analytical techniques, could be applied as a new reliable and versatile tool for simultaneous protease detection.

Author contributions

Petra Jedináková: synthesis, basic fluorescent characterization, enzymatic studies, writing the manuscript. David Milićević: synthesis, basic fluorescent characterization. Zuzana Barbuščáková: synthesis and analysis of the prepared compounds. Martin Kubala: Advanced fluorescent measurements. Jan Hlaváč: management of the project, writing the article.

Conflicts of interest

There are no conflicts to declare.

Data availability

The data supporting this article have been included as part of the SI. See DOI: **https://doi.org/10.1039/d5ra03163j**.

Acknowledgements

The authors are grateful to the Faculty of Science, Palacký University, for financial support.

Notes and references

1 C. López-Otín and J. S. Bond, *J. Biol. Chem.*, 2008, **283**, 30433–30437.
2 M. Verdoes and S. H. L. Verhelst, *Biochim. Biophys. Acta, Proteins Proteomics*, 2016, **1864**, 130–142.
3 M. Rodriguez-Rios, A. Megia-Fernandez, D. J. Norman and M. Bradley, *Chem. Soc. Rev.*, 2022, **51**, 2081–2120.
4 I. L. H. Ong and K. L. Yang, *Analyst*, 2017, **142**, 1867–1881.
5 B. Dasmahapatra, *Biotechnol. Adv.*, 1997, **15**, 728.
6 J. Zhang, X. Chai, X. P. He, H. J. Kim, J. Yoon and H. Tian, *Chem. Soc. Rev.*, 2019, **48**, 683–722.
7 X. Wu, J. Simone, D. Hewgill, R. Siegel, P. E. Lipsky and L. He, *Cytometry, Part A*, 2006, **69**, 477–486.
8 S. Y. Li, L. H. Liu, H. Cheng, B. Li, W. X. Qiu and X. Z. Zhang, *Chem. Commun.*, 2015, **51**, 14520–14523.
9 H. Cheng, S. Y. Li, H. R. Zheng, C. X. Li, B. R. Xie, K. W. Chen, B. Li and X. Z. Zhang, *Anal. Chem.*, 2017, **89**, 4349–4354.
10 A. Megia-Fernandez, B. Mills, C. Michels, S. V. Chankeshwara, N. Krstajić, C. Haslett, K. Dhaliwal and M. Bradley, *Org. Biomol. Chem.*, 2018, **16**, 8056–8063.
11 Y. Cheng, R. M. Borum, A. E. Clark, Z. Jin, C. Moore, P. Fajtová, A. J. O'Donoghue, A. F. Carlin and J. V. Jokerst, *Angew. Chem., Int. Ed.*, 2022, **61**, e202113617.
12 Y. Okorochenkova, M. Porubský, S. Benická and J. Hlaváč, *Chem. Commun.*, 2018, **54**, 7589–7592.
13 M. Porubský, E. Řezníčková, S. Křupková, V. Kryštof and J. Hlaváč, *Bioorg. Chem.*, 2022, **129**, 106151.
14 D. Milićević and J. Hlaváč, *ACS Omega*, 2024, **9**, 17481–17490.

15 D. Milićević and J. Hlaváč, *RSC Adv.*, 2022, **12**, 28780–28787.
16 W. R. Algar, A. P. Malanoski, K. Susumu, M. H. Stewart, N. Hildebrandt and I. L. Medintz, *Anal. Chem.*, 2012, **84**, 10136–10146.
17 W. R. Algar, M. G. Ancona, A. P. Malanoski, K. Susumu and I. L. Medintz, *ACS Nano*, 2012, **6**, 11044–11058.
18 E. Petryayeva and W. R. Algar, *Anal. Chem.*, 2014, **86**, 3195–3202.
19 M. Massey, H. Kim, E. M. Conroy and W. R. Algar, *J. Phys. Chem. C*, 2017, **121**, 13345–13356.
20 P. Das, S. Ganguly, P. K. Marvi, M. Sherazee, X. Tang, S. Srinivasan and A. R. Rajabzadeh, *Adv. Mater.*, 2024, **36**, 1–20.
21 H. Y. Tsai, H. Kim, M. Massey, K. D. Krause and W. R. Algar, *Methods Appl. Fluoresc.*, 2019, **7**, 042001.
22 Y. Huang, M. Shi, K. Hu, S. Zhao, X. Lu, Z. F. Chen, J. Chen and H. Liang, *J. Mater. Chem. B*, 2013, **1**, 3470–3476.
23 J. Xu, L. Fang, M. Shi, Y. Huang, L. Yao, S. Zhao, L. Zhang and H. Liang, *Chem. Commun.*, 2019, **55**, 1651–1654.
24 X. Michalet, F. F. Pinaud, L. A. Bentolila, J. M. Tsay, S. Doose, J. J. Li, G. Sundaresan, A. M. Wu, S. S. Gambhir and S. Weiss, *Science*, 2005, **307**, 538–544.
25 G. He, D. Guo, C. He, X. Zhang, X. Zhao and C. Duan, *Angew. Chem., Int. Ed.*, 2009, **48**, 6132–6135.
26 Y. J. Gong, X. B. Zhang, G. J. Mao, L. Su, H. M. Meng, W. Tan, S. Feng and G. Zhang, *Chem. Sci.*, 2016, **7**, 2275–2285.
27 V. Krchňák and V. Paděra, *Bioorg. Med. Chem. Lett.*, 1998, **8**, 3261–3264.
28 G. Jones, W. R. Jackson, C. Y. Choi and W. R. Bergmark, *J. Phys. Chem.*, 1985, **89**, 294–300.
29 J. H. Brannon and D. Magde, *J. Phys. Chem.*, 1978, **82**, 705–709.